



# Development of Targeted Magnetic Bentonite Nanocarrier for the Delivery of 5-Fluorouracil

Nagajothi Dharmalingam<sup>1</sup>, Vanangamudi Arumugasamy<sup>1,\*</sup>, Rajan Mariappan<sup>2</sup>, Kevin Kumar Vijayakumar<sup>3</sup>, Shakila Harshavardhan<sup>3</sup>

<sup>1</sup> Ayya Nadar Janaki Ammal College (Affiliated to Madurai Kamaraj University), Department of Chemistry, Sivakasi - 626124, India; nagajothid@gmail.com (N.D.); sudhakanivanangamudi@gmail.com (V.A.);

<sup>2</sup> Biomaterials in Medicinal Chemistry Laboratory, Department of Natural Products Chemistry, School of Chemistry, Madurai Kamaraj University, Madurai 625021, Tamil Nadu, India; rajanm153.chem@mkuniversity.org (R.M.);

<sup>3</sup> Department of Molecular Microbiology, School of Biotechnology, Madurai Kamaraj University, Madurai 625021, Tamil Nadu, India; kevinumarv.2008@gmail.com (K.K.V.); mohanshakila@yahoo.com (S.H.);

\* Correspondence: sudhakanivanangamudi@gmail.com (V.A.);

Scopus Author ID 6507127640

Received: 5.08.2022; Accepted: 23.09.2022; Published: 6.01.2023

**Abstract:** The research aims to develop a novel 5-fluorouracil (5-FU) loaded magnetite bentonite nanocarrier for targeted anticancer drug delivery to obtain the most favorable therapeutic response and offer effective and safe *in vitro* anticancer treatment. The Iron oxide was functionalized in the bentonite clay through an electrostatic interaction reaction to form magnetite bentonite nanoparticles. The targeting ligand of biotin bonded with the cross-linker of glutathione to form biotinylated glutathione in magnetite bentonites. The synthesized nanocarrier system is characterized by using different analytical techniques. The average particle size of the carrier and 5-FU loaded carrier was 31nm from the Scherrer equation. In SEM analysis, 5-FU loaded and unloaded carriers form sheet & needle-like and flower-like structures, respectively. The 5-fluorouracil in the magnetite bentonite nanocarriers was observed at 59.0 % loading capacity and 72.13% encapsulation efficiency. *In vitro* cytotoxicity effects of 5-FU loaded nanocarrier were studied in lung cancer cells (A549). The synthesized 5-FU-loaded nanocarriers exhibited increased cytotoxicity and apoptosis in the lung A549 cells. Hence, the results suggest that the 5-FUloaded magnetite bentonite possesses strong *in vitro* anticancer and antioxidant activity as a potential drug carrier for lung cancer therapy.

**Keywords:** bentonite; biotin; 5-fluorouracil; lung cancer; magnetic; nanocarrier.

© 2023 by the authors. This article is an open-access article distributed under the terms and conditions of the Creative Commons Attribution (CC BY) license (<https://creativecommons.org/licenses/by/4.0/>).

## 1. Introduction

Developing potential antitumor agents with a low toxicological profile against healthy cells is still one of the most significant challenges against many diseases [1]. Cancer is a potential danger to life in the present era. Among different cancers, lung cancer is a leading cause of mortality and morbidity worldwide [2, 3]. The potential toxicity of anticancer drugs in cancer treatment also fosters damage to normal cells. It becomes a major concern in synthesizing a suitable and targeted drug carrier. Nanotechnology in the medical field aids with the positive preparation of viable drug carriers with a positive sign of target-oriented drug release [4, 5]. Drug carriers play an important role in promoting the efficacy of the drug. Drug delivery and the drug-encapsulated nanoparticles enhanced the drug delivery to the target cells and reduced the drug's toxicity to the non-target sites [6 - 8]. The clay minerals and drugs administer the absorption capability and reduce it by interacting with the drug. As a result, these interactions are utilized to achieve technological and biopharmaceutical advantages such

as controlled drug release. The entire properties of clay nanomaterials make them suitable nanocarriers for perfect loading and the controlled release of various drugs such as antibiotics, anticancer, antioxidants, anti-inflammatories, etc. [9, 10]. Bentonites are multifunctional, with unique swelling and adsorption properties. They have been applied to the drug delivery system to overcome the drug disadvantages such as low solubility levels, short biological half-life, and poor and low bioavailability.

Bentonite clay is efficient and has high potential as a drug delivery system for using hydrophilic drugs with good loading capacity and constant release [11, 12]. Surface modification can be done to enhance the property of bentonite clay. One of the best modifications includes the surface coating of clays with metal oxide nanoparticles to increase the surface area and alter basic properties [13, 14]. Magnetic nanoparticles, drug-loaded, magnetically controlled, and targeted to diseased tissues, are being studied as prospective therapy [15, 16]. The primary advantage of a site-targeted anticancer drug delivery system is the drug release at the tumor site, which minimizes the level of toxicity to normal healthy cells [17, 18]. In current decades vitamin-like drug targeting is a positive and novel model for carrying anticancer drugs to cancer target sites. Biotin is a most effective anticancer drug targeting agent that improves cell uptake and enhances carrier shift across potential cancer cells [19, 20].

Furthermore, glutathione acts as a strong intracellular antioxidant and plays a vital role in shielding the cells from oxidative stress. Biotin receptors have over-functioned on the cancer cell surface compared with normal cells [21, 22]. It remains a major need in cancer treatment to achieve an efficient drug delivery system for 5-fluorouracil (5-FU) to develop its effectiveness. Indeed, The magnetite bentonite targeted drug carrier helps to develop the biocompatibility of 5-FU to decrease the side effects and enhance the efficiency of 5-FU cancer treatment [23, 24]. The anticancer-encapsulated magnetite bentonite nanocarrier in the drug delivery system has attained excellent biocompatibility, effective drug loading efficiency, good stability, and storage [25, 26].

## 2. Material and Methods

### 2.1. Materials.

Bentonite Clay, Biotin, Glutathione, Ferric chloride, Ferrous sulfate, 5-Fluorouracil, N hydroxy succinimide (NHS), 1-Ethyl-3-(3-dimethyl aminopropyl)carbodiimide(EDC) 3-(4,dimethylthiazol-2-yl)-2,5 diphenyltetrazolium bromide (MTT) and artesunate were purchased from Sigma Aldrich Co., Ltd, Mumbai, India. *N, N*-dimethylformamide (DMF), Dimethyl sulfoxide (DMSO), Methanol (MeOH), and sulfuric acid were purchased from Merck Co., Ltd, Mumbai, India. Double distilled water was used throughout the experimental reactions and analysis.

### 2.2. Preparation of magnetite bentonite (MB) nanoparticles.

The fabrication of magnetite bentonite nanoparticles is followed by two steps using the previously reported technique [15]. Briefly, 2.5milligram of ferrous sulfate ( $\text{FeSO}_4$ ) was added to 3milligram of bentonite clay in 50mL distilled water with stirring for 3 h at 950rpm and further added 10mL of 25% ammonia solution with a continuous stirring for three hours at 80°C under a nitrogen atmosphere. After finishing the reaction, the product was washed with distilled water five or six times to remove any unreacted species and then dried at 60°C. In the

second step, the prepared iron nanoparticles were added to the bentonite, followed by the addition of concentrated hydrochloric acid to activate this process to maintain pH4. The mixture was refluxed at 65°C for 2hrs with continuous stirring. The final product was washed with distilled water, dried, and then calcinated at 400°C for 3hrs to form the final product whitish powder.

### 2.3. Fabrication of biotin-glutathione (BG) targeting ligand.

The synthesis of Biotin-glutathione was carried out according to a previously reported method [27]. Briefly, biotin-glutathione was prepared using the standard amide band formation method using coupling reagents like EDC and NHS. 600mg of biotin in 5mL DMF, followed by adding coupling reagents (420mg of EDC & 250mg of NHS), stirring 15min for activation of the carboxylic group, and then further stirred for one hour at room temperature. After one hour, maintain the pH 6 (using acetic acid & sodium hydroxide solution) and add 1 gram of glutathione in 5mL DMF with continuous stirring for 24hrs. The precipitate was filtered and washed with diethyl ether, purified using dialysis against distilled water for 48 hours, and dried at 40°C.

### 2.4. Magnetite bentonite/biotin-glutathione (MB/BG) nanocarrier preparation.

Magnetite Bentonite/Biotin-Glutathione (MB/BG) nanocarrier prepared by an aqueous solution of biotin-glutathione was added dropwise into the aqueous solution of magnetite bentonite nanoparticles under the vigorous stirring in a magnetic stirrer for 12 h at room temperature. Then, the product was washed with deionized water and dried.

### 2.5. Fabrication of 5-Fluorouracil (5-FU) loaded Magnetite Bentonite/Biotin-Glutathione (MB/BG) nanocarriers.

An aqueous solution of 5mg 5-fluorouracil was added to the aqueous solution of 10 mg of magnetite bentonite nanocarrier and stirred for 24hrs at room temperature. The product was collected and washed by ultracentrifugation at 3,000 rpm for 20 min to remove the supernatant solution of the boundless drug molecule. Further, the encapsulation and loading capacity of the drug-loaded nanocarrier was evaluated with the help of UV irradiation and applied for biological applications. Figure 1 demonstrates the schematic diagram of the synthesized 5FU-loaded magnetic bentonite nanocarrier.

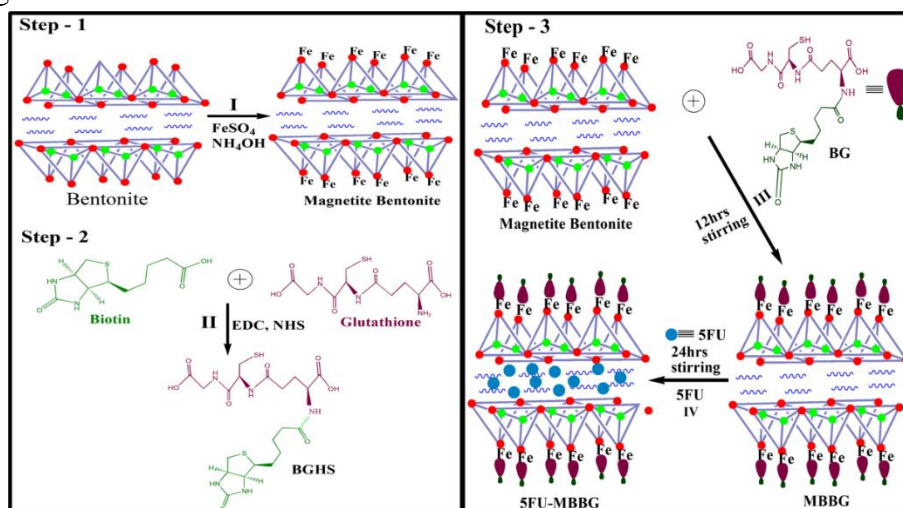


**Figure 1.** Synthesis of 5-FU loaded magnetic bentonite nanocarrier.

### 3. Result and Discussion

#### 3.1. FTIR analysis.

The functional group of prepared nanocarriers with their components was investigated through FTIR analysis, and it was investigated to find the formation of magnetite bentonite (MB), biotin glutathione (BG), magnetite bentonite-biotin glutathione (MB/BG) and 5-Fluorouracil (5-FU) loaded MB/BG as shown in Figure 2. Magnetite bentonite is good bioavailability and biodegradable nature. Figure 2a shows that the peaks at  $461\text{cm}^{-1}$  indicate the presence of possible charge interaction of Fe-O stretching frequency that represents the successful interaction of bentonite and iron, which is correlated to the previous report of Sharma *et al.* [15]. Biotin is widely used in the delivery of anticancer agents due to its high tumor tissue specificity with over-expressed biotin-specific receptors [28]. Figure 2b shows the FTIR spectrum of biotinylated glutathione, and absorbance band  $1649\text{cm}^{-1}$  indicates the amide  $-\text{CONH}$  group in both carrier and drug-loaded carrier bands. It represents the presence of the biotinylated glutathione in the carrier, and these are similar to Kavitha *et al.* and Morral-Ruiz G *et al.* [21, 27, 29]. Figure 2c demonstrates the interaction of magnetite bentonite and biotinylated glutathione at the O-Fe-O stretching frequency of  $554\text{cm}^{-1}$ . Figure 2d indicates the pure drug of 5 fluorouracil and the peaks at  $3468\text{cm}^{-1}$ ,  $1649\text{cm}^{-1}$ , and  $639\text{cm}^{-1}$ , respectively. The presence of two new peaks,  $788\text{cm}^{-1}$ , and  $2913\text{cm}^{-1}$ , in Figure 2e, represents the successful loading of 5-FU in the magnetic bentonite nanocarrier and the departure of a peak at  $957\text{cm}^{-1}$  loading of 5-FU. The peak of  $788\text{cm}^{-1}$  denotes the presence of CF-CH vibration, and  $3000\text{-}3500\text{cm}^{-1}$  denotes the presence of excess F groups in 5-FU as related to the studies of Nivetha *et al.* [24, 25].

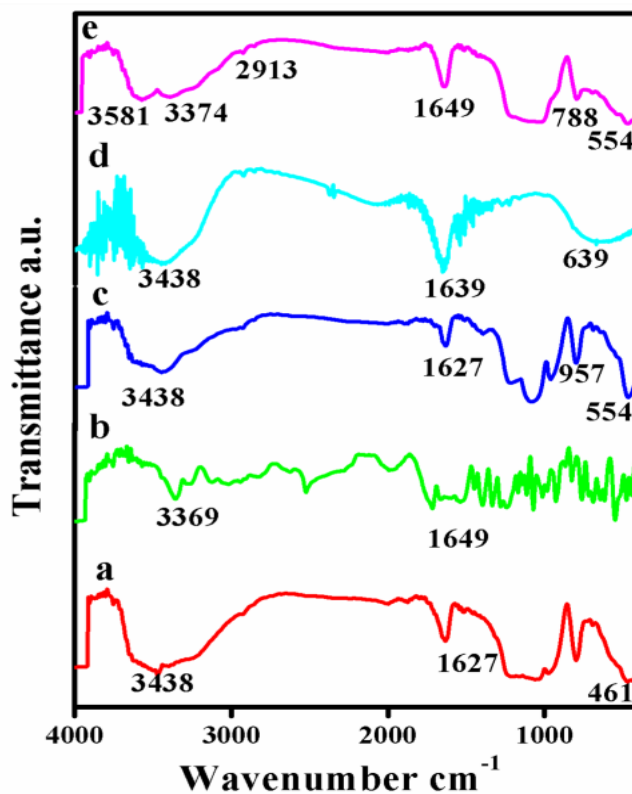


**Figure 2.** FTIR Spectral analysis of the (a) Magnetite Bentonite nanoparticles (MB); (b) Biotin-Glutathione targeting ligand (BG); (c) Magnetite Bentonite/Biotin-Glutathione (MB/BG) targeted nanocarrier; (d) 5-fluorouracil; (e) 5-fluorouracil loaded Magnetite Bentonite/ Biotin-Glutathione (5-FU loaded MB/BG) nanocarriers.

3.2. XRD analysis.

The crystalline phase differentiation of 5-FU loaded and unloaded magnetite bentonite nanocarrier systems was examined by X-ray diffraction spectroscopy. Figure 3 shows Magnetite bentonite X-ray diffraction patterns, Biotinylated Glutathione, MB/BG nanocarrier, and 5-FU loaded MB/BG nanocarrier. Figure 3(a) represents the diffractogram of bentonite-modified magnetic nanoparticles at  $2\theta$  values of  $20.81^\circ$ ,  $27^\circ$ ,  $36.71^\circ$ ,  $42.44^\circ$ ,  $60^\circ$  and  $68^\circ$ , which refer to the magnetite bentonite having a cubic structure. The presence of bentonite is represented at a high-intensity peak of nearly  $27^\circ$  with the Miller index (220). The diffraction peaks  $36.71^\circ$ ,  $42.44^\circ$ , and  $60^\circ$  with indices of planes (311), (400), and (440) indicate the presence of magnetic iron oxide. Anitha *et al.* also reported a similar crystalline nature of magnetite bentonite nanoparticles [25]. Figure 3(b) depicts the XRD pattern of biotinylated glutathione, and the structurally modified biotin with glutathione diffraction was observed. The main peak of crystalline biotin appeared at  $11.82^\circ$ ,  $17.44^\circ$ ,  $18.96^\circ$ ,  $21.13^\circ$ ,  $22.87^\circ$ ,  $28.49^\circ$ , and  $35.65^\circ$  respectively. The glutathione peaks are observed at  $22.44^\circ$ ,  $30.88^\circ$  and  $33.9^\circ$  angles, closely related to previously reported literature [30]. Figure 3(c) represents the XRD pattern of the MB/BG nanocarrier and shows the modified magnetite bentonite with biotinylated glutathione targeted ligands. After modification, the magnetite bentonite peaks are still present and have some new biotinylated glutathione peaks ( $17.44^\circ$ ,  $18.96^\circ$ ,  $21.13^\circ$ ,  $33.9^\circ$ ), which denotes the presence of magnetite bentonite core modified with biotin-targeted ligands. The free 5-FU crystalline nature is confirmed and was previously reported by Ezekiel, C. I *et al.* [31]. Figure 3(d) indicates the 5-FU loaded MB/BG nanocarrier; it is slightly changed in position, and the intensity of peaks is observed. The characteristic diffraction peak of 5-FU appeared at  $2\theta = 27^\circ$ , and no apparent characteristic diffraction peak of 5-FU-MB/BG appeared at  $2\theta = 27^\circ$ . The result showed that the 5-FU drug carrier had intercalated in the interlayer of magnetite bentonite. The drug was a small crystal type of MB/BG nanocarrier without damaging the layered structure nanocarrier. Mingliang Ge *et al.* also demonstrate the related report using a 5FU-loaded magadiite nanocarrier [32]. The new peak of  $16.1^\circ$  also denotes the presence of crystalline 5-FUinnanocarriers. The intensity change from 24 to 32 confirmed the encapsulation of 5-FU and demonstrated the strong crystallinity of the encapsulated 5-FU magnetite bentonite nanocarrier.

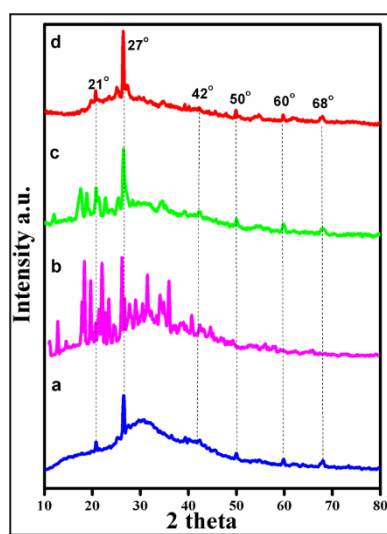


**Figure 3.** XRD analysis of Magnetite Bentonite nanocarrier and drug-loaded carrier. (a) Magnetite Bentonite Nanoparticles; (b) Biotin-Glutathione targeted ligand; (c) Magnetite Bentonite/ Biotin-Glutathione targeted nanocarrier; (d) 5-FU loaded Bentonite/ Biotin-Glutathione nanocarrier.

3.3. Particle size analysis.

The particle size and size distribution of loaded and unloaded nanocarriers were obtained from the particle size analyzer. The results in the form of a particle-size histogram are shown in Figure 4. The solid line represents the log-normal distribution best fit to the obtained histogram. The average particle size of the prepared magnetite bentonite nanocarrier was 31 nm, whereas the diameter range of 5-FU loaded magnetite bentonite nanocarrier was 34 nm in the results of the XRD Scherrer equation. The particle size's loaded 5-FU molecule on the magnetite bentonite surface was enlarged. The polydispersity for the magnetite bentonite nanocarrier before and after loading with 5-FU was 0.34 and 0.322, correspondingly. The 0.3 or below polydispersity indicated homogenous distribution of the nanocarrier. Due to the tiny size of the nanocarrier, it easily penetrates the target cancer cells.

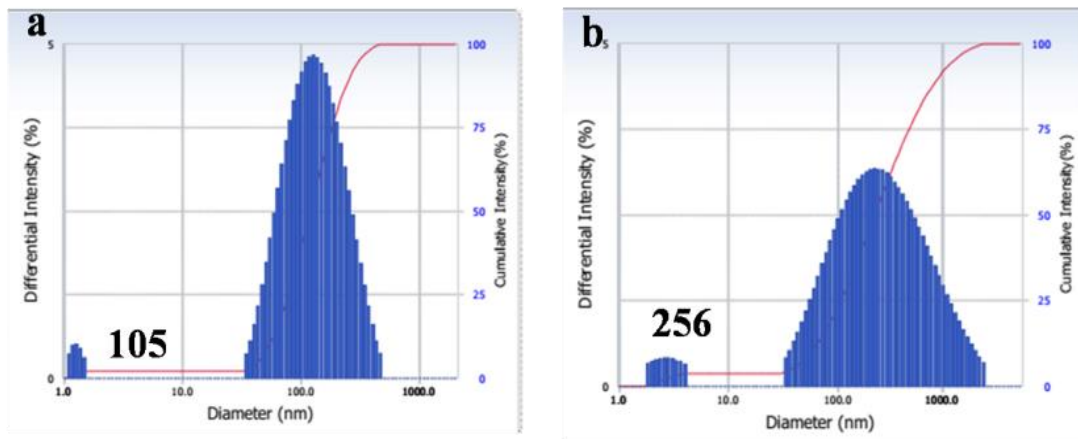


**Figure 4.** Particle size analysis (a) 5-FU loaded magnetite bentonite nanocarriers and (b) 5-FU unloaded magnetite bentonite nanocarriers.

3.4. Scanning electron microscopy analysis (SEM).

The imaging study studied surface morphology and microstructure of MB, BG, MB/BG, and 5-FU loaded MB/BG, as shown in Figure 5. Figure 5(a) represents the morphology of the magnetite bentonite.

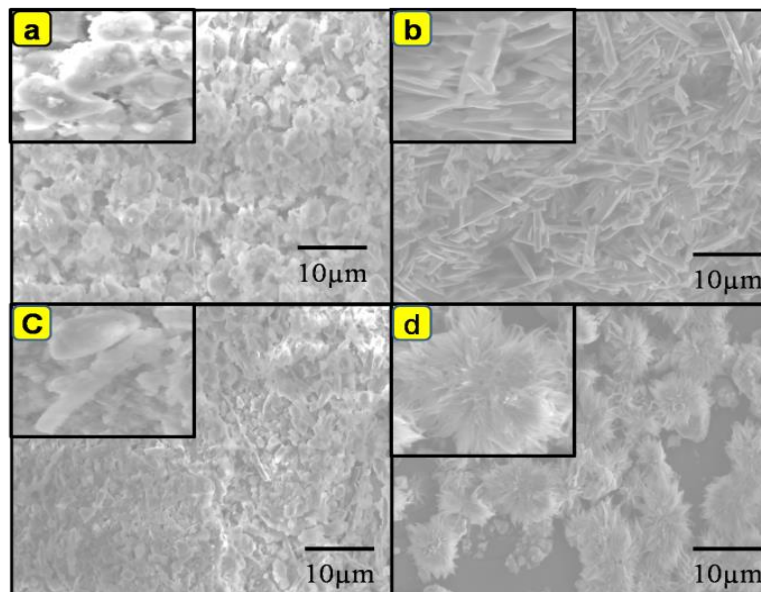


**Figure 5.** SEM image of magnetite bentonite-based carrier and drug-loaded carrier. (a) Magnetite bentonite nanoparticles; (b) Biotin-Glutathione targeting ligand; (c) Magnetite bentonite-based targeted nanocarrier; (d) 5-Fluorouracil loaded magnetite bentonite nanocarrier.

It has a rough and flakes-like crystal surface with a porous surface due to impregnated magnetite nanoparticles on the clay surface [14]. Figure 5(b) represents that the biotinylated glutathione targeted ligand has a rod-like structure with a nonporous surface. In addition, the magnetite bentonite and biotinylated glutathione targeted ligand in Figure 5(c) shows mixed flakes and rod-like structures due to the magnetite bentonite and biotinylated interaction of glutathione. Figure 5(d) shows that the flower-like structure of the 5-FU loaded carrier and the 5-FU small crystals were loaded to the interlayer of the carrier. The loading of 5-FU in the carrier enhanced the interspacing of the magnetite bentonite-based carrier.

### 3.5. Radical scavenging activity.

The antioxidant activity of 5-Fluorouracil loaded and unloaded magnetite bentonite nanocarrier was determined using a radical scavenging assay free from DPPH in Spectrophotometric methods. The antioxidant activity of 5-FU loaded and unloaded various concentrations of samples evaluated the nanocarrier, and the sample concentration was increased to enhance the antioxidant activity. The results indicate the diphenylpicrylhydrazyl radical scavenging of a maximum of 55.26% at 450 $\mu\text{g}/\text{mL}$  for both 5-FU loaded and unloaded nanocarriers with a minimum of 3.63% for 5-FU unloaded carrier and 7.60% for 5-FU loaded carrier at 50 $\mu\text{g}/\text{mL}$ . Du *et al.* reported nanocarriers are useful tools in antioxidant activity in the future. The results also proved that there is good antioxidant activity of 5-FU loaded and unloaded nanocarriers [33].

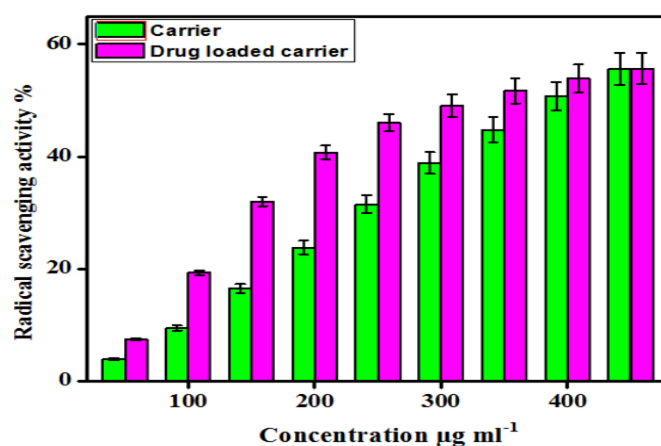


**Figure 6.** Radical scavenging activity of 5-FU loaded and unloaded nanocarrier.

### 3.6. MTT Assay/Cell viability analysis.

The toxicity of 5FU loaded and unloaded nanocarrier on A549 cells was determined by MTT assay. It was tested for 24 h against a lung cancer cell line (A549) with different concentrations (25, 50, 75,100  $\mu\text{g}/\text{mL}$ ), as shown in Figures 7 & 8. Figure 7 shows that 5fluorouracil-loaded biotin-targeted magnetite bentonite nanocarriers have higher cytotoxic effects (24%) at 150  $\mu\text{g}/\text{mL}$  compared with low concentrations of these nanocarriers. The surface change is an important determinant of cytotoxic activity because the negatively charged loaded nanocarrier interacts with the positively charged cell membrane. Furthermore, the  $\text{IC}_{50}$  of the 5fluorouracil-loaded biotin-targeted magnetite bentonite nanocarrier is 85  $\mu\text{g}/\text{mL}$ . However,  $\text{IC}_{50}$  values of the 5FU loaded and unloaded nanocarrier are over (92% and 70%) at 50  $\mu\text{g}/\text{mL}$  for A549 cell lines, demonstrating the high biocompatibility of the carrier material. This result reveals the drawbacks of using the drug alone in chemotherapy treatment without a

drug delivery system. As expected, the 5-FU loaded nanocarrier shows high toxicity against the cancer cell lines, which is correlated to the previous report of Nivethaa *et al.* and Teow *et al.* [34, 35].

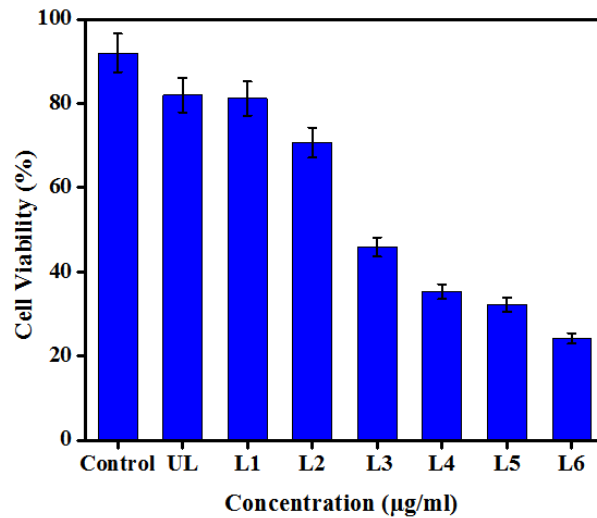


**Figure 7.** Cytotoxicity in A549 cells treated with 5-FU loaded MB/BG nanocarrier for 24h. UL - Unloaded carrier (50µg/mL), L1- 5-FU loaded carrier (25µg/mL), L2- 5-FU loaded carrier (50µg/mL), L3- 5-FU loaded carrier (75µg/mL), L4- 5-FU loaded carrier (100µg/mL), L5- 5-FU loaded carrier (125µg/mL), L6- 5-FU loaded carrier (150µg/mL).

### 3.7. *In vitro* Morphological Studies.

*In vitro* morphological changes of A549 cells were observed by inverted light microscopy, and the results are given in Figure 8. An extreme morphological change was observed in A549 cells after 24h treatment. Compared with the control group, the 5-FU-loaded nanocarrier-treated A549 cells demonstrate intrinsic cell damage and shrinkage. Figure 8 represents the morphological changes of 5fluorouracil-loaded biotin-targeted magnetite bentonite nanocarrier on A549 cancer cells. There are no considerable differences in control & unloaded nanocarrier-treated A549 cancer cells. The 5fluorouracil loaded nanocarrier (25-150 µg/mL) treated cancer cells show loss of intact membrane and cell-cell communication, condensed and detached from the culture plate.

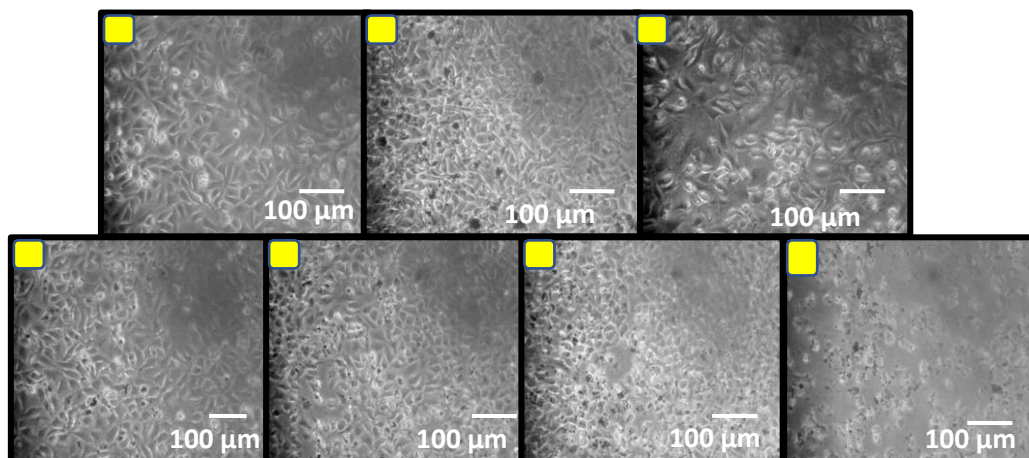


**Figure 8.** Morphological Changes in A549 cells treated with 5-FU loaded MB/BG nanocarrier for 24h. (a) Control (50µg/mL); (b) Unloaded carrier (50µg/mL); (c) 5-Fluorouracil (50µg/mL); (d) 5-FU loaded carrier (25µg/mL); (e) 5-FU loaded carrier (50µg/mL); (f) 5-FU loaded carrier (75µg/mL); (g) 5-FU loaded carrier (100µg/mL).

The results concentration of nanocarriers increases with potential changes in A549 cell morphology, such as decreased cell density, increased necrosis, cell death, cell detachment, cell shrinkage, and formation of apoptotic bodies. These studies are similar to the reported literature by Pan *et al.* [36, 37].

### 3.8. Encapsulation efficiency and *in vitro* drug release studies.

The efficient drug carrier design and development depend on two important parameters: encapsulation efficiency and loading capacity of drug carrier systems. The UV-Vis spectrum of the drug-loaded nanocarrier shows the 5-FU absorbance peak at 269 nm. The loading capacity and encapsulation efficiency of 5-FU were obtained at 59% and 72.13%. These results indicate the anticancer drugs were successfully encapsulated on magnetite bentonite nanocarrier. Finally, high encapsulating and loading efficiency bounded carriers will help improve the *in vitro* drug release application [38].

The rate of drug delivery of 5-FU from the magnetic bentonite nanocarrier was investigated at three different pH levels, 2.8, 5.5 & 7.4, at room temperature, and the results are demonstrated in Figure 9. The UV-Visible spectroscopy analysis recorded a cumulative drug release nature of the 5-FU loaded Magnetite bentonite nanocarrier. At 30hrs investigations, a maximum of 99.99 % of the 5-FU release rate was observed in acidic pH 2.8. The interacted 5-FU molecule was easily cleavable under acidic conditions. The acidic medium from the Magnetite-bentonite carrier is an efficient drug to release nanocarrier systems for biomedical applications. Figure 9 shows the drug release pattern of a 5-FU loaded Magnetite bentonite nanocarrier; the release rate of 5-FU at pH-5.5 is 25.85 %, and pH-7.4 is 32.84% drug release with the 30hrs intervals. Finally, the acidic condition was the most suitable environment for delivering 5-Fluorouracil drugs in cancer cells. Thus, the results indicate that the 5-FU drug in the nanocarrier is well protected from the physiological environment, and release behavior from the nanocarrier is modulated by changes in environmental pH media, meaning that the nanocarrier can be used effectively in the targeted treatment of cancer cells. Notably, the drug release behavior from the 5-FU loaded Magnetite bentonite nanocarrier is similar to previously reported literature by Yusefi *et al.* and Ruman *et al.* [39 - 42], which have shown that at pH 2.8, 5-FU is released more rapidly than it is at pH 5.5, 7.4.

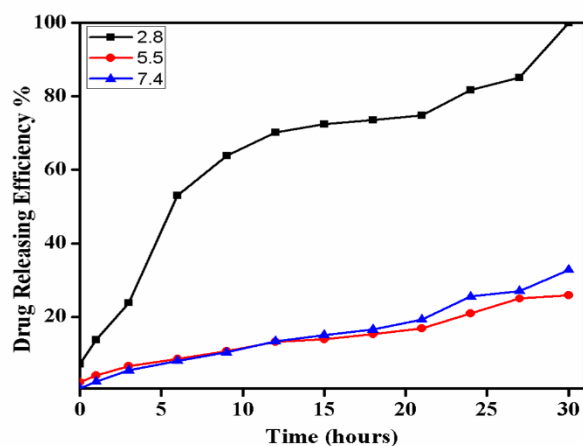


Figure 9. Drug releasing efficiency of 5-Fluorouracil loaded Magnetite bentonite nanocarrier.

## 4. Conclusions

The synthesized magnetite bentonite was successfully loaded with 5-Fluorouracil through physical and chemical interaction in this research work. The magnetite bentonite, <https://biointerfaceresearch.com/>

further conjugated with a biotin-targeted ligand using glutathione, acts as a cross-linking agent to attain a site-specific drug delivery. These nanocarriers showed an efficient loading capacity of 5-Fluorouracil, a good adsorbent, and targeted drug release as an anticancer; this observation is important as it can overcome the conventional release of the anticancer drug to target places. A high drug release rate was observed in acidic pH conditions in intracellular environments works. The *in vitro* studies indicated that the targeted and synergetic therapy for cancer treatment showed significant cell death of cancer cells. The results suggested that magnetite bentonite nanocarrier could be targeted for drug delivery to improve cancer therapy's therapeutic efficiency.

## Funding

No funding.

## Acknowledgments

The authors acknowledge Ayya Nadar Janaki Ammal College, Sivakasi, and Madurai Kamaraj University, Madurai, for supporting this work.

## Conflicts of Interest

The authors declare no conflict of interest.

## References

1. Ciaffaglione, V.; Modica, M. N.; Pittala, V.; Romeo, G.; Salerno, L.; Intagliata, S. Mutual Prodrugs of 5-Fluorouracil: From a Classic Chemotherapeutic Agent to Novel Potential Anticancer Drugs. *Chem. Med. Chem.* **2021**, *16*, 3496–3512, <https://doi.org/10.1002/cmdc.202100473>.
2. Bray, F.; Ferlay, J.; Soerjomataram, I.; Siegel, R.L.; Torre, L.A.; Jemal, A. Global cancer statistics 2018: GLOBOCAN estimates of incidence and mortality worldwide for 36 cancers in 185 countries *CA: A Cancer J. Clin.* **2018**, *68*, 394–424, <https://doi.org/10.3322/caac.21492>.
3. Rastogi, A.; Yadav, K.; Mishra, A.; Singh, M.; Chaudhary, S.; Manohar, R.; Parmar, A. Early diagnosis of lung cancer using the magnetic nanoparticles-integrated systems. *Nanotechnology Reviews* **2022**, *11*, 544–574, <https://doi.org/10.1515/ntrev-2022-0032>.
4. Siegel, R.L.; Miller, K.D.; Fuchs, H.E. Cancer Statistics. *CA: A Cancer J. Clin.* **2022**, *72*, 7–33, <https://doi.org/10.3322/caac.21708>.
5. Kamazani, F.M.; Nematalahi, F.S.; Siadat, S.D.; Pornour, M.; Sheikhpour, M. A success targeted nano delivery to lung cancer cells with multi-walled carbon nanotubes conjugated to bromocriptine. *Scientific Reports* **2021**, *11*, 24419, <https://doi.org/10.1038/s41598-021-03031-2>.
6. Wang, J.; Zhou, T.; Liu, Y.; Chen, S.; Yu, Z. Application of Nanoparticles in the Treatment of Lung Cancer with Emphasis on Receptors. *Front. Pharmacol.* **2022**, *12*, 781425, <https://doi.org/10.3389/fphar.2021.781425>.
7. Ghafouri-Fard, S.; Abak, A.; Tondro Anamag, F.; Shoorei, H.; Fattahi, F.; Javadinia, S.A.; Basiri, A.; Taheri, M. 5-Fluorouracil: A Narrative Review of on the Role of Regulatory Mechanisms in Driving Resistance to This Chemotherapeutic Agent. *Front. Oncol.* **2021**, *11*, 658636, <https://doi.org/10.3389/fonc.2021.658636>.
8. Reneeta, N.P.; Thiyonila, B.; Aathmanathan, V.S.; Ramya, T.; Chandrasekar, P.; Subramanian, N.; Prajapati, V.K.; Krishnan, M. Encapsulation and systemic delivery of 5-fluorouracil conjugated with silkworm pupa derived protein nanoparticles for experimental lymphoma cancer. *Bioconjugate Chemistry* **2018**, *29*, 2994–3009, <https://doi.org/10.1021/acs.bioconjchem.8b00404>.
9. Khatoun, N.; Chu, M.; Zhou, C. Nanoclay-based drug delivery systems and their therapeutic potentials. *J. Mater. Chem. B.* **2020**, *8*, 7335–7351, <https://doi.org/10.1039/D0TB01031F>.
10. Delori, A.; Eddleston, M.D.; Jones, W. Cocrystals of 5-Fluorouracil. *CrystEngComm* **2013**, *15*, 73–77, <https://doi.org/10.1039/c2ce26147b>.

11. Gong, Z.; Liao, L.; Lv, G.; Wang, X. A simple method for physical purification of bentonite. *Applied Clay Science* **2016**, *119*, 294–300, <https://doi.org/10.1016/j.clay.2015.10.031>.
12. Martsouka, F.; Papagiannopoulos, K.; Hatziantoniou, S.; Barlog, M.; Lagiopoulos, G.; Tatoulis, T.; Tekerlekopoulou, A.G.; Lampropoulou, P.; Papoulis, D. The Antimicrobial Properties of Modified Pharmaceutical Bentonite with Zinc and Copper. *Pharmaceutics* **2021**, *13*, 1190, <https://doi.org/10.3390/pharmaceutics13081190>.
13. Sonawane, G.H.; Patil, S.P.; Shrivastava, V.S. Photocatalytic degradation of safranin by ZnO–bentonite: photodegradation versus adsorbability. *J. Inst. Eng. (India): Series E* **2017**, *98*, 55–63, <https://doi.org/10.1007/s40034-016-0089-1>.
14. Lubis, S.; Sheilatina; Sitompulm, D.W. Photocatalytic degradation of indigo carmine dye using  $\alpha$ -Fe<sub>2</sub>O<sub>3</sub>/bentonite nanocomposites prepared by mechanochemical synthesis. *IOP Conf. Ser: Mater. Sci. Eng.* **2019**, *509*, 012142, <https://doi.org/10.1088/1757-899X/509/1/012142>.
15. Sharma, P.; Kumari, S.; Ghosh, D. *et al.* Capping agent-induced variation of physicochemical and biological properties of  $\alpha$ -Fe<sub>2</sub>O<sub>3</sub> nanoparticles. *Mater. Chem. Phys.* **2021**, *258*, 123899, <https://doi.org/10.1016/j.matchemphys.2020.123899>.
16. Luo, Z.; Du, H. Prospect of different types of magnetic nanoparticles in stem cell therapy. *Stem. Cell. Rev. Rep.* **2020**, *16*, 675–683, <https://doi.org/10.1007/s12015-020-09966-9>.
17. Fraguas-Sánchez, A.I.; Fernández-Carballido, A.; Delie, F.; Cohen, M.; Martin-Sabroso, C.; Mezzanzanica, D.; Figini, M.; Satta, A.; Torres-Suárez, A.I. Enhancing ovarian cancer conventional chemotherapy through the combination with cannabidiol loaded microparticles. *Eur. J. Pharm. Biopharm.* **2020**, *154*, 246–258, <https://doi.org/10.1016/j.ejpb.2020.07.008>.
18. Vinothini, K.; Kumar, N.; Munusamy, M.A.; Alarfaj, A.A.; Rajan, M. Development of biotin molecule targeted cancer cell drug delivery of doxorubicin-loaded  $\kappa$ -carrageenan grafted graphene oxide nanocarrier. *Materials Science & Engineering C* **2019**, *100*, 676–687, <https://doi.org/10.1016/j.msec.2019.03.011>.
19. Lu, N-N.; Xie, M.; Wang, J.; Lv, S-W.; Yi, J-S.; Dong, W-G.; Huang, W-H. Biotin Triggered Decomposable Immunomagnetic Beads for Capture and Release of the Circulating Tumor Cells. *ACS Appl. Mater. Interfaces* **2015**, *7*, 8817–8826, <https://doi.org/10.1021/acsami.5b01397>.
20. Mauro, N.; Scialabba, C.; Cavallaro, G.; Licciardi, M.; Giammona, G. Biotin-Containing Reduced Graphene Oxide-Based Nanosystem as a Multi-effect Anticancer Agent: Combining Hyperthermia with Targeted Chemotherapy. *Biomacromolecules* **2015**, *16*, 2766–2775, <https://doi.org/10.1021/acs.biomac.5b00705>.
21. Kavita; Singh, K.; Kumar, S.; Bhatti, H.S. Glutathione-assisted synthesis of star-shaped zinc oxide nanostructures and their photoluminescence behaviour. *J. Lumin.* **2014**, *149*, 112–117, <https://doi.org/10.1016/j.jlumin.2014.01.001>.
22. Balan, V.; Dodi, G.; Mihai, C.T.; Serban, A.M.; Ursachi, V.C. Biotinylated chitosan macromolecule based nanosystems: A review from chemical design to biological targets. *International Journal of Biological Macromolecules* **2021**, *188*, 82–93, <https://doi.org/10.1016/j.ijbiomac.2021.07.197>.
23. Shi, Q.; Anishiya Chella Daisy, E.R.; Yang, G.; Zhang, J.; Mickymaray, S.; Alfaiz, F-A.; Paramasivam, A.; Rajan, M. Multi-featured guar gum armed drug delivery system for the delivery of ofloxacin drug to treat ophthalmic diseases. *Arabian Journal of Chemistry* **2021**, *14*, 5, 103118, <https://doi.org/10.1016/j.arabjc.2021.103118>.
24. Nivethaa, E.A.K.; Dhanavel, S.; Rebekah, A.; Narayanan, V.; Stephen, A. A comparative study of 5-Fluorouracil release from chitosan/silver and chitosan/silver/MWCNT nanocomposites and their cytotoxicity towards MCF-7. *Materials Science and Engineering: C* **2016**, *66*, 244–250, <https://doi.org/10.1016/j.msec.2016.04.080>.
25. Anitha, A.; Chennazhi, K.P.; Nair, S.V.; Jayakumar, R. 5-Fluorouracil loaded N, O carboxymethyl chitosan nanoparticles as an anticancer nanomedicine for breast cancer. *J. Biomed. Nanotechnol.* **2012**, *8*, 29–42, <https://doi.org/10.1166/jbn.2012.1365>.
26. Mateus, A.; Torres, J.; Marimon-Bolivar, W.; Pulgarín, L. Implementation of magnetic bentonite in food industry wastewater treatment for reuse in agricultural irrigation. *Water Resources and Industry* **2021**, *26*, 100154, <https://doi.org/10.1016/j.wri.2021.100154>.
27. Qurat-ul-Ain. Free Radical Scavenging and Cytotoxic Activities of Substituted Pyrimidines. *Cancer. Ther. Oncol. Int. J.* **2020**, *16*, 555940, <https://doi.org/10.19080/CTOIJ.2020.16.555940>.
28. Parashar, P.; Tripathi, C.B.; Arya, M.; Kanoujia, J.; Singh, M.; Yadav, A.; Kumar, A.; Guleria, A.; Saraf, S.A. RETRACTED ARTICLE: Biotinylated naringenin intensified anticancer effect of gefitinib in urethane-induced lung cancer in rats: favourable modulation of apoptotic regulators and serum metabolomics. *Artificial*

- Cells, Nanomedicine, and Biotechnology.* 2018, 46, 598-610, <https://doi.org/10.1080/21691401.2018.1505738>.
29. Morral-Ruíz, G.; Melgar-Lesmes, P.; López-Vicente, A.; Solans, C.; García-Celma, M.J. Biotinylated polyurethane-urea nanoparticles for targeted theranostics in human hepatocellular carcinoma. *Nano. Res.* **2015**, 8, 1729–1745, <https://doi.org/10.1007/s12274-014-0678-6>.
  30. Arockia Jency, D.; Sathyavathi, K.; Mahalingam, U.; Ramasamy, P. Enhanced bioactivity of Fe<sub>3</sub>O<sub>4</sub>-Au nanocomposites - A comparative antibacterial study. *Materials Letters* **2020**, 258, 126795, <https://doi.org/10.1016/j.matlet.2019.126795>.
  31. Ezekiel, C.I.; Bapolisi, A.M.; Walker, R.B.; Krause, R.W.M. Ultrasound-Triggered Release of 5 Fluorouracil from Soy Lecithin Echogenic Liposomes. *Pharmaceutics* **2021**, 13, 821, <https://doi.org/10.3390/pharmaceutics13060821>.
  32. Ge, M.; Tang, W.; Du, M.; Liang, G.; Hu, G.; Jahangir Alam, S.M. Research on 5-fluorouracil as a drug carrier materials with its *in vitro* release properties on organically modified magadiite. *European Journal of Pharmaceutical Sciences* **2019**, 130, 44–53, <https://doi.org/10.1016/j.ejps.2019.01.017>.
  33. Du, L.; Li, J.; Chen, C.; Liu, Y. Nanocarrier: a potential tool for future antioxidant therapy. *Free radical research* **2014**, 48, 1061–1069, <https://doi.org/10.3109/10715762.2014.924625>.
  34. Nivethaa, E.A.K.; Dhanavel, S.; Narayanan, V.; Arul Vasu, C.; Stephen, A. An *in vitro* cytotoxicity study of 5-fluorouracil encapsulated chitosan/gold nanocomposites towards MCF-7 cells. *RSC Adv.* **2015**, 5, 1024-1032, <https://doi.org/10.1039/C4RA11615A>.
  35. Yusefi, M.; Chan, H.-Y.; Teow, S.-Y.; Kia, P.; Soon, M.L.-K.; Sidik, N.A.B.C.; Shameli, K. 5-Fluorouracil Encapsulated Chitosan-Cellulose Fiber Bionanocomposites: Synthesis, Characterization and *In vitro* Analysis towards Colorectal Cancer Cells. *Nanomaterials* **2021**, 11, 1691, <https://doi.org/10.3390/nano11071691>.
  36. Pan, X.; Zhang, X.; Sun, H.; Zhang, J.; Yan, M.; Zhang, H. Autophagy Inhibition Promotes 5-Fluorouracil-Induced Apoptosis by Stimulating ROS Formation in Human Non-Small Cell Lung Cancer A549 Cells. *PLoS ONE* **2013**, 8, e56679, <https://doi.org/10.1371/journal.pone.0056679>.
  37. Nasonovs, A.; Garcia-Diaz, M.; Bogenhagen, D.F. A549 cells contain enlarged mitochondria with independently functional clustered mtDNA nucleoids. *PLoS ONE* **2021**, 16, e0249047, <https://doi.org/10.1371/journal.pone.0249047>.
  38. Wu, C.F.; Wu, C.Y.; Chiou, R.Y.; Yang, W.C.; Lin, C.F.; Wang, C.M.; Hou, P.H.; Lin, T.C.; Kuo, C.Y.; Chang, G.R. The Anti-Cancer Effects of a Zotarolimus and 5-Fluorouracil Combination Treatment on A549 Cell-Derived Tumors in BALB/c Nude Mice. *International Journal of Molecular Sciences* **2021**, 22, 4562, <https://doi.org/10.3390/ijms22094562>.
  39. Yusefi, M.; Shameli, K.; Hedayatnasab, Z.; Teow, S.-Y.; Ismail, U.N.; Azlan, C.A.; Rasit Ali, R. Green synthesis of Fe<sub>3</sub>O<sub>4</sub> nanoparticles for hyperthermia, magnetic resonance imaging and 5-fluorouracil carrier in potential colorectal cancer treatment. *Res. on Chem. Intermed.* **2021**, 47, 1789-1808, <https://doi.org/10.1007/s11164-020-04388-1>.
  40. Ruman, U.; Buskaran, K.; Pastorin, G.; Masarudin, M.J.; Fakurazi, S.; Hussein, M.Z. Synthesis and characterization of chitosan-based nano delivery systems to enhance the anticancer effect of sorafenib drug in hepatocellular carcinoma and colorectal adenocarcinoma cells. *Nanomaterials* **2021**, 11, 497, <https://doi.org/10.3390/nano11020497>.
  41. Park, J.-H.; Shin, H.-J.; Kim, M. H.; Kim, J.-S.; Kang, N.; Lee, J.-Y.; Kim, T.-K.; Lee, J. I.; Kim, D.-D. Application of montmorillonite in bentonite as a pharmaceutical excipient in drug delivery systems. *Int. J. Pharm. Invest.* **2016**, 46, 363–375, <https://doi.org/10.1007/s40005-016-0258-8>.
  42. Al-Obaidi, H.; Granger, A.; Hibbard, T.; Opeanwo, S. Pulmonary Drug Delivery of Antimicrobials and Anticancer Drugs Using Solid Dispersions. *Pharmaceutics* **2021**, 13, 1056, <https://doi.org/10.3390/pharmaceutics13071056>.